ELSEVIER

Thermochimica Acta 313 (1998) 83–95

thermochimica acta

Thermal degradation kinetics of epoxy–anhydride resins: I. Influence of a silica filler

S. Montserrat, J. Málek[1,*], P. Colomer

Laboratori de Termodinamica ETSEIT, Departament de Maquines i Motors Termics Universitat Politecnica de Catalunya, Carrer de Colom 11, E-08222 Terrassa, Spain

Received 7 July 1997; received in revised form 23 October 1997; accepted 21 November 1997

Abstract

Thermal degradation kinetics of epoxy–anhydride resins has been studied by thermogravimetry in both, isothermal and non-isothermal conditions. It was found that the kinetics of thermal degradation can be fairly described by a simple reaction-order model. The calculated kinetic parameters, E_a and n, are considerably lower for pure resin than for resin containing silica filler. Therefore, the addition of silica filler increases thermal degradation rate of the resin. A difference was also observed between the set of kinetic parameters obtained by kinetic analysis of isothermal and non-isothermal data, particularly with respect to the activation energy. © 1998 Elsevier Science B.V.

Keywords: Epoxy resins; Kinetics; Thermal degradation

1. Introduction

Thermogravimetric analysis is a technique widely used to study the thermal degradation of polymeric materials which is affected by their structure, the type of curing agents and additives. Different methods have been proposed to study the kinetics of such process either by isothermal or non-isothermal conditions, see Refs. [1,2]. Special interest pertains the analysis in non-isothermal conditions [3–5]. Some of these methods have been applied to a thermal degradation of epoxy resins [6,7]

The main objective of this work is to study the kinetics of thermal degradation of an epoxy resin in isothermal and non-isothermal conditions using an analysis based on the methodology introduced by Málek [8,9] for analysis of calorimetric data. Kinetic parameters are obtained from both isothermal and non-isothermal data and the limits of applicability of a simple kinetic equation are analyzed. The effect of a silica filler on the degradation kinetics is also studied.

2. Theory

In TG experiments the change of the sample mass is registered as a function of temperature (non-isothermal experiments) or time (isothermal experiment). The fractional extent of reaction is

*Corresponding author. Tel.: 00 42 4047461; fax: 00 42 4048400; e-mail: malek@pol.upce.cz

[1]Permanent address: Joint Laboratory of Solid State Chemistry, Academy of Sciences of the Czech Republic and University of Pardubice, Studentská 84, PARDUBICE 530 09, Czech Republic.

PII S0040-6031(97)00482-6

expressed as

$$\alpha = \frac{m_0 - m}{m_0 - m_\infty} \quad (1)$$

where m is an actual mass at time t (or at temperature T), m_0 the initial sample mass and m_∞ the mass at the end of isothermal or non-isothermal experiments.

The differential kinetic equation can be expressed as [1]

$$\left(\frac{d\alpha}{dt}\right) = Ae^{-x} f(\alpha) \quad (2)$$

where A is a pre-exponential factor of the Arrhenius type rate constant and x the reduced apparent activation energy ($x = E_a/RT$). The function $f(\alpha)$ in Eq. (2) is an analytical expression describing the kinetic model of the studied thermal decomposition process (Table 1). The mutual correlation of Arrhenius kinetic parameters (apparent activation energy and pre-exponential factor) and kinetic model does not allow an accurate kinetic analysis to be performed by using only one experimental TG [1,10]. This problem can be solved by calculating the apparent activation energy from several isothermal (or non-isothermal) experiments and by determining the most probable kinetic model, as described in Sections 2.1 and 2.2.

2.1. Isothermal kinetics

By integration of Eq. (2) in isothermal conditions the following equation is obtained:

$$g(\alpha) = \int_0^\alpha \frac{d\alpha}{f(\alpha)} = Ae^{-x} \cdot t \quad (3)$$

The apparent activation energy of the decomposition process in isothermal conditions can be calculated by isoconversional method which follows from logarithmic form of Eq. (3):

$$\ln t = \ln[g(\alpha)/A] + \frac{E_a}{RT} \quad (4)$$

The slope of $\ln t$ vs. $1/T$ for the same value of α gives the value of apparent activation energy. This procedure can be repeated for various values of α. Therefore, the method provides a check of invariance of E_a with respect to α in the $0.3<\alpha<0.7$ range, which is one of basic assumptions in kinetic analysis of TG data.

Combining Eqs. (2) and (3) a new function $Z(\alpha)$ can be defined:

$$Z(\alpha) = \left(\frac{d\alpha}{dt}\right) t = f(\alpha)g(\alpha) \quad (5)$$

For practical reasons this function is normalized within the (0, 1) interval. It was shown by Málek [9] that the maximum of this function (usually labeled α_p^∞) has characteristic values for basic kinetic models as shown in Table 1. It is seen that the α_p^∞ is constant for D2, D3, D4 and JMA(m) model. On the other hand, it depends on particular value of kinetic exponent for the RO(n) or SB(M, N) model. Therefore, the function $Z(\alpha)$ is useful for basic classification of possible kinetic model but it is not sufficient for an unambiguous determination of true kinetic model function $f(\alpha)$. In isothermal conditions, however, the term Ae^{-x} in Eq. (2) is constant and the reaction rate ($d\alpha/dt$) is proportional to the $f(\alpha)$ function:

$$Y(\alpha) = \left(\frac{d\alpha}{dt}\right) \approx f(\alpha) \quad (6)$$

Therefore, if the reaction rate is plotted as a function α its shape corresponds to the $f(\alpha)$ function. It is

Table 1
The kinetic models and maxima of the $z(\alpha)$ function (α_p^∞) and $y(\alpha)$ function (α_M)

Model	Symbol	$f(\alpha)$	α_p^∞	α_M
Reaction order	RO(n)	$(1-\alpha)^n$	$1-n^{1/(1-n)}$	0
Johnson–Mehl–Avrami	JMA(m>1)	$m(1-\alpha)[-\ln(1-\alpha)]^{1-1/m}$	0.633	$1-\exp(1/m-1)$
Šesták–Berggren	SB(M,N) [a]	$\alpha^M(1-\alpha)^N$	$(0,\alpha_p)$	M/(M+N)
2D-diffusion	D2	$-1/\ln(1-\alpha)$	0.834	0
Jander eqn.	D3	$3(1-\alpha)^{2/3}/2[1-(1-\alpha)^{1/3}]$	0.704	0
Ginstling–Brounshtein	D4	$3/2[(1-\alpha)^{-1/3}-1]$	0.776	0

[a] The SB model is valid for 0<M<1 ([14]).

convenient to normalize the $Y(\alpha)$ plot within (0, 1) interval. The shape of this plot is characteristic for each kinetic model and it can be used as a diagnostic probe for kinetic model determination. The following rules can be formulated [8–10] in this respect:

1. If the $Y(\alpha)$ function has a maximum at $\alpha_M=0$ then it can be convex, linear or concave. Convex dependence corresponds to RO(n<1) model, linear dependence to the JMA(m=1) or RO(n=1) model (these two models are formally identical) and concave dependence to the JMA(m<1), D2, D3, D4 and RO(n>1) model.
2. If the $Y(\alpha)$ function exhibit a maximum in interval $\alpha_M\in(0, \alpha_p)$ (where α_p is the fractional extent of reaction at the maximum $d\alpha/dt$) then it corresponds to the SB(M, N) or JMA(m>1) model. The mathematical condition for these maxima are shown in Table 1.

Thus, the shape of both $Y(\alpha)=(d\alpha/dt)$ and $Z(\alpha)$ function can be used conveniently for the determination of the most probable kinetic model [9]. It is seen that in isothermal conditions the kinetic model can easily be determined by simple transformation of experimental data. The kinetic exponent for the RO(n) model can be obtained from the maximum, α_p^∞, of the $Z(\alpha)$ function and the kinetic exponents of JMA(m>1) and SB(M,N) are obtained from maximum, α_M, of the $Y(\alpha)$ function (Table 1).

2.2. Non-isothermal kinetics

The apparent activation energy of the decomposition process in non-isothermal conditions can be calculated by isoconversional method [11] which follows from logarithmic form of Eq. (2):

$$\ln\left(\frac{d\alpha}{dt}\right) = \ln[Af(\alpha)] - \frac{E_a}{RT} \tag{7}$$

The slope of $\ln(d\alpha/dt)$ vs. $1/T$ for the same value of α gives the value apparent activation energy. Similarly, as described in Section 2.1, the apparent activation energy can be calculated for various values of α and in this way it is possible to verify an invariance of E_a with respect to α.

In non-isothermal conditions when the temperature rises at a constant heating rate β, then we obtain after integration of Eq. (2) the following equation [1,9]:

$$g(\alpha) = Ae^{-x}\left[\frac{T}{\beta}\pi(x)\right] \tag{8}$$

where $\pi(x)$ is an approximation of the temperature integral. There are various expression of the $\pi(x)$ term in the literature [1]. The rational expression of Senum and Yang [12] gives sufficiently accurate results:

$$\pi(x) = \frac{x^3 + 18x^2 + 86x + 96}{x^4 + 20x^3 + 120x^2 + 240x + 120} \tag{9}$$

Combining Eqs. (2) and (8), we can obtain following expression for the $z(\alpha)$ function in non-isothermal conditions [9]:

$$z(\alpha) = \left(\frac{d\alpha}{dt}\right)\left[\frac{T}{\beta}\pi(x)\right] = f(\alpha)g(\alpha) \tag{10}$$

Recently, it was found by numerical simulations [13] that the term in brackets in Eq. (10) is proportional to T^2. Therefore, the expression for the $z(\alpha)$ function can be substantially simplified:

$$z(\alpha) \approx \left(\frac{d\alpha}{dt}\right)T^2 \tag{11}$$

Using Eq. (11), the $z(\alpha)$ function can be obtained by a very simple transformation of experimental data just by multiplying measured reaction rate ($d\alpha/dt$) by T^2 and then normalizing within the (0,1) interval. Similarly, as in isothermal conditions this can be done without the knowledge of any kinetic parameter. On the other hand, in non-isothermal conditions the reaction rate ($d\alpha/dt$) is not directly proportional to $f(\alpha)$ as the term Ae^{-x} is not constant. However, the shape of $f(\alpha)$ function can be obtained from the $y(\alpha)$ function defined as [9]:

$$y(\alpha) = \left(\frac{d\alpha}{dt}\right)e^x = Af(\alpha) \tag{12}$$

This function is usually normalized also within (0, 1) interval. It has the same mathematical properties as those for isothermal conditions. However, as evident from Eq. (12) for calculation of $y(\alpha)$ function it is necessary to know the apparent activation energy in the case of non-isothermal conditions.

3. Experimental

The epoxy resin studied was a commercial epoxy resin based on diglycidyl ether of bisphenol A (DGEBA), named Araldite CY225 from CIBA-GEIGY (epoxy equivalent of 121.3 g/equiv) cured by a cyclic carboxylic anhydride derived from methyl tetrahydrophthalic anhydride, hardener CY225 (CIBA-GEIGY) with accelerator incorporated. The epoxy resin and the hardener were mixed in the weight ratio of 100:80, and vigorously stirred at room temperature for ca. 20 min. The mixture was then degassed under vacuum and cured isothermally at 130°C for 8 h. This fully cured epoxy will be referred to as epoxy CY. The other resin used has the same mode of preparation but with the addition of silica (CIBA-GEIGY filler Q5) in the weight ratio of epoxy:silica:hardener=100:125:80. The latter resin will be referred as epoxy CYSI. The curing conditions of epoxy CYSI were the same as in CY.

The thermogravimetric measurements were carried out by a TG-50 thermobalance coupled to a METTLER TA4000 instrument. Non-isothermal experiments were performed at heating rate of 2.5, 5, 10, 15 and 20 K/min. In the isothermal experiments, the furnace was heated up to the desired temperature. Then the sample was introduced, and the weight loss was measured over a period between 5 and 15 h depending on the experiment temperature. In both cases, powdered samples of ca. 7 mg were used and a nitrogen gas flow of 200 ml/min was permanently applied.

4. Results and discussion

4.1. Isothermal degradation kinetics

Thermal degradation in isothermal conditions was studied in the $340^{\circ}C \leq T \leq 380^{\circ}C$ range for the CY sample and $320^{\circ}C \leq T \leq 360^{\circ}C$ for the CYSI sample. These conditions are determined by the given TG instrument as well as by the kinetics of the thermal degradation process of epoxy resins. Outside the specified temperature ranges, it is quite difficult to obtain reliable TG data. At higher temperatures, the thermal degradation is so fast that the initial part of TG curve might be lost during the instrument settling period. In contrast, at lower temperatures the thermal degradation becomes very slow and it is not so easy to determine correctly the relative mass loss corresponding to completely degraded sample.

Typical isothermal TG curves for the CY sample and the CYSI sample at 360°C normalized with respect to the initial sample weight are shown in Fig. 1. Broken lines show relative mass loss corresponding to completely degraded samples. For the CY sample, it was taken at 380°C after 10 h but practically same value is also obtained for lower temperatures at 370 and 360°C. In contrast, the constant value was not reached for comparable time and temperatures in the case of the CYSI sample. In this case, the relative mass loss corresponding to completely degraded sample was taken from non-isothermal experiment at 2.5 K/min. Fig. 1 shows that the CY sample loses a weight fraction of 0.84, while the CYSI sample loses a fraction 0.37, against the expected loss of ca. 0.50, according to the composition of this resin with a content of 41% silica filler. This fact may suggests that the filler may be promoting a different char-forming reaction in nitrogen atmosphere. Using these limiting values the TG curve can easily be transformed to $\alpha(t)$ plots and then analyzed by isoconversional method (Eq. (4)) as described in Section 2.1. This method enables plotting of apparent activation energy E_a as shown in Fig. 2. Any point in this figure (corresponding to E_a for constant α) was obtained from the slope of $\ln t$ vs. $1/T$ plot within the certain error limits (specified by bars). As mentioned in Section 2, the apparent activation energy should be invariant with respect to α in the $0.3<\alpha<0.7$ range. In fact the value of E_a increases with fractional conversion being higher and more α dependent for the CYSI sample. It should be pointed out that a more pronounced E_a–α plot may be a consequence of more complex mechanism controlling thermal degradation process. An inspection of Fig. 2 shows ca. 7% variation for the CY sample and ca. 13% for the CYSI sample. These changes are higher than the average error limit which corresponds to 2% for the CY sample and 4% for the CYSI sample, respectively. Therefore, average values of apparent activation energy determined in the $0.3<\alpha<0.7$ range are 173 ± 12 kJ/mol for the CY sample and 202 ± 26 kJ/mol for the CYSI sample.

As anticipated in Section 2.1, for reliable kinetic analysis of thermogravimetric data in isothermal con-

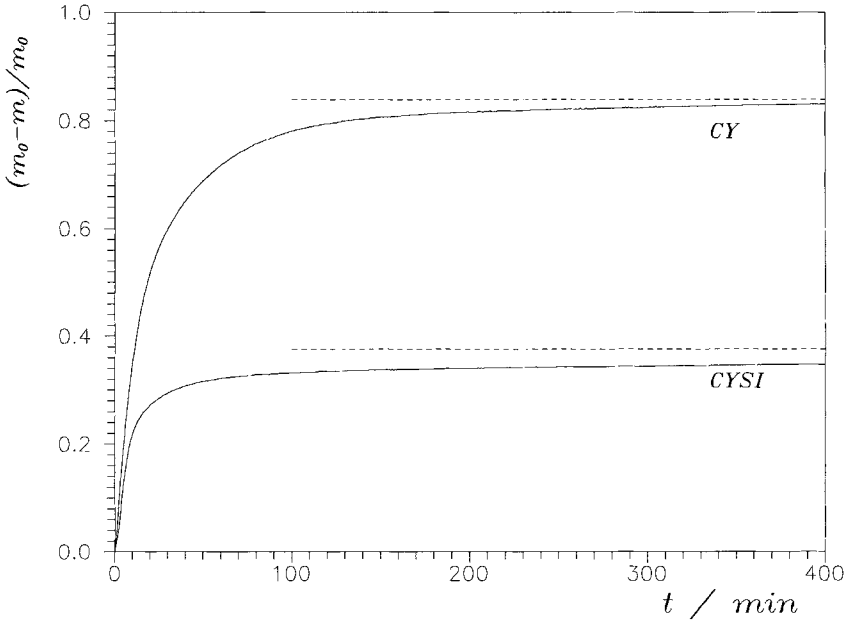

Fig. 1. Isothermal TG curves for the CY and CYSI sample (T=360°C) normalized to the initial sample weight. Broken lines show the limits used for calculation of fractional conversion α.

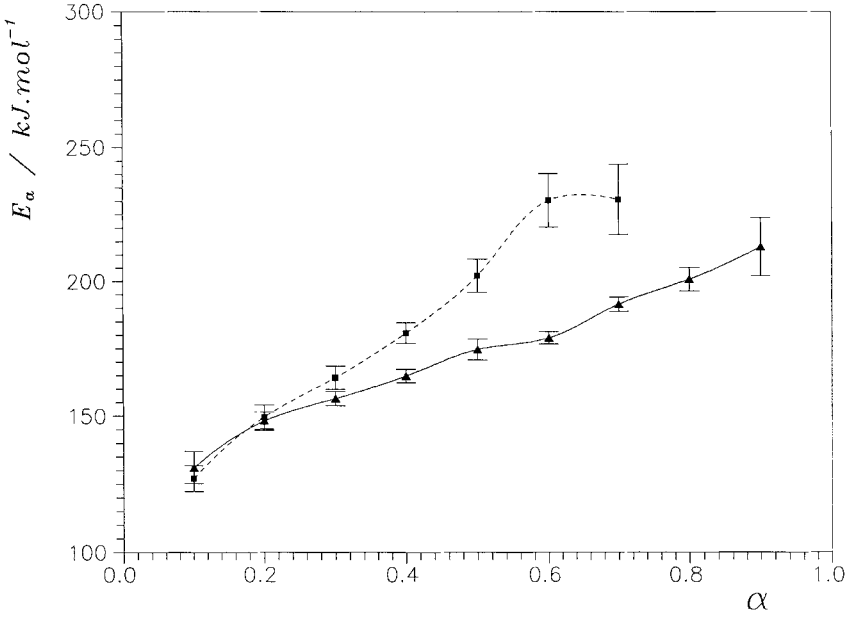

Fig. 2. The apparent activation energy calculated from isothermal TG data plotted as a function of fractional conversion for the CY sample (▲) and the CYSI sample (■). The points were calculated by the isoconversional method using Eq. (4) and the lines are drawn as guides for the eye.

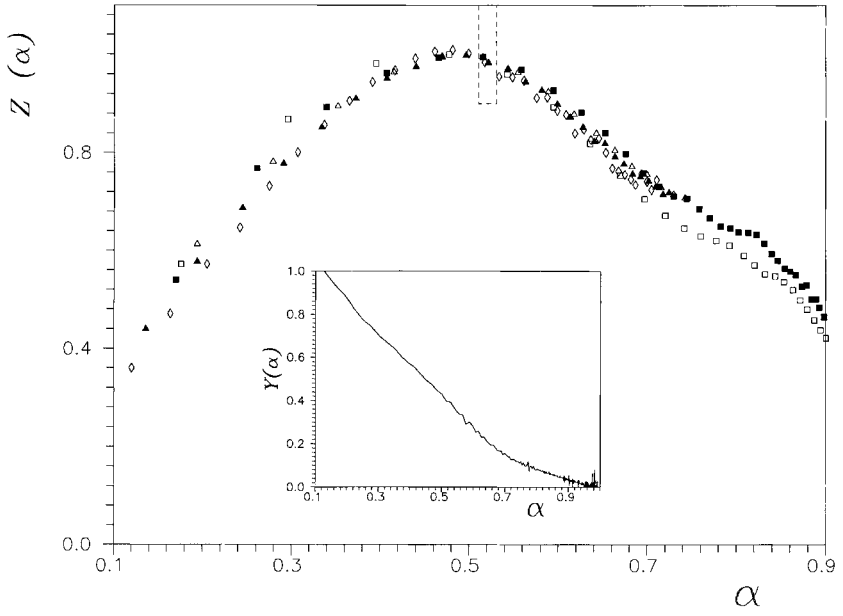

Fig. 3. The $Z(\alpha)$ functions for the CY sample calculated using Eq. (5) for various isothermal experiments: (□) 380°C; (■) 370°C; (△) 360°C; (▲) 350°C; (◇) 340°C. Broken lines correspond to theoretical maxima calculated using Eq. (14). The inset shows the $Y(\alpha)$ function for the same sample (T=360°C) calculated using Eq. (6).

ditions it is necessary to determine kinetic model. This can be easily done by using the $Y(\alpha)$ and $Z(\alpha)$ functions. These functions were obtained from isothermal experimental ($d\alpha/dt$) data using Eqs. (5) and (6) and they are shown in Figs. 3 and 4 for CY and CYSI sample, respectively. The shape of the $Z(\alpha)$ function is practically invariant with respect to temperature. In both cases, the $Y(\alpha)$ function is concave (see inset of Fig. 3) and the maxima of $Z(\alpha)$ function is $\alpha_p^{\infty} < 0.5$. The most probable kinetic model is, therefore, RO(n>1) model. Knowing the kinetic model the equation for isothermal $\alpha(t)$ curve is obtained from Eq. (3). For the RO model it can be written in the following form:

$$\alpha(t) = 1 - [1 - t(1-n)\mathrm{A}e^{-x}]^{1/(1-n)} \qquad (13)$$

The value of reduced activation energy is constant in isothermal conditions (x=E_a/RT) and it can easily be calculated for average value of apparent activation energy obtained by isoconversional analysis (see above). The values of parameters n and A can then be obtained by non-linear regression of experimental data. The average values obtained for both CY sample (340°C≤T≤380°C) and CYSI sample (320°C≤T≤360°C) are shown in Table 2. About 20% increase in the value of pre-exponential factor for the CYSI sample corresponds to the slight increase of activation energy in comparison with the CY sample. Nevertheless, the value of kinetic exponent n is considerably higher for the CYSI than for the CY sample and this change cannot be explained only by the differences in activation energy and it seems that the filler may be promoting quite different mechanism of thermal

Table 2
The kinetic parameters obtained by non-linear regression of isothermal data using Eq. (13) and constant value of activation energy (173 kJ/mol for the CY sample and 202 kJ/mol for the CYSI sample

	CY		CYSI	
T/°C	n	ln(A/min)	n	ln(A/min)
380	1.47	29.98	—	—
370	1.50	29.95	—	—
360	1.50	30.05	2.73	36.74
350	1.80	30.20	2.93	36.65
340	1.96	30.22	3.20	36.90
330	—	—	3.20	36.90
320	—	—	3.36	36.69

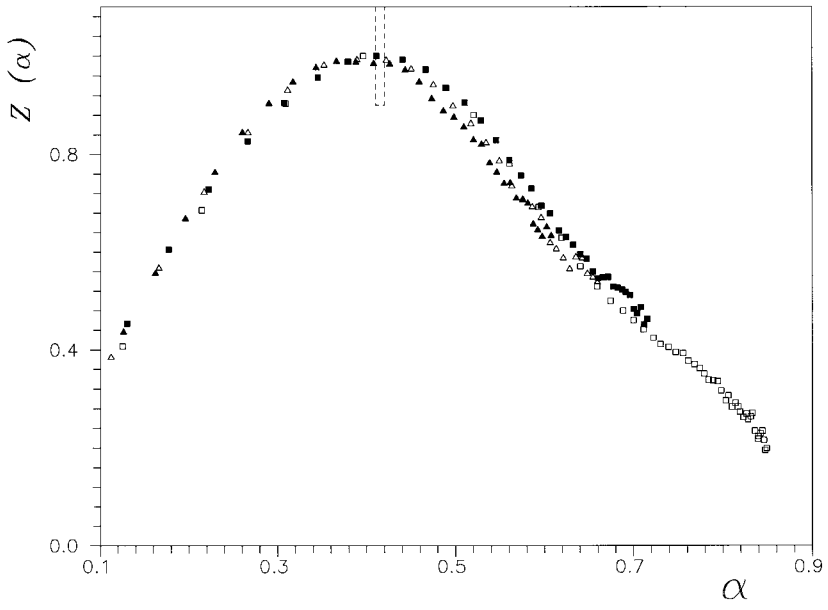

Fig. 4. The $Z(\alpha)$ functions for the CYSI sample calculated using Eq. (5) for various isothermal experiments: (□) 360°C; (■) 350°C; (△) 340°C; (▲) 330°C. Broken lines correspond to theoretical maxima calculated using Eq. (14).

degradation process. The maximum of the $Z(\alpha)$ function for the RO model can be expressed as a function of the kinetic exponent:

$$\alpha_p^{\infty} = 1 - n^{1/(1-n)} \quad (14)$$

Using this equation the limiting values of α_p^{∞} were calculated for the kinetic exponent (within the error limits) determined from data shown in Table 2. These calculated limiting values are compared (broken lines) with the experimental $Z(\alpha)$ function (points) in Figs. 3 and 4. There is quite good agreement between maxima of experimental $Z(\alpha)$ functions and values calculated from Eq. (14).

Figs. 5 and 6 show the comparison of experimental data (points) and calculated $\alpha(t)$ plots for the CY and CYSI sample (full lines). The $\alpha(t)$ curves were calculated using Eq. (13) for the kinetic parameters shown in Table 2. There is quite good agreement between experimental data and the prediction of the RO model. Some discrepancies are observed only for the CYSI sample at higher temperatures (T>340°C). These discrepancies can probably be explained to be a consequence of higher variation of E_a with α for the CYSI sample. Strictly speaking, Eq. (13) is valid only for a constant value of apparent activation energy. This assumption is evidently not fulfilled when a silica filler is incorporated into the epoxy resin. The thermal degradation rate is considerably higher for the CYSI sample in the temperature range studied. This observation is consistent with higher value of both the activation energy and the kinetic exponent n for the CYSI sample.

4.2. Non-isothermal degradation kinetics

The thermogravimetric curves in non-isothermal conditions were obtained at different heating rates ranging from 2.5 to 20 K/min. Typical non-isothermal DTG curves for the CY and CYSI sample are shown in Fig. 7 for heating rate 5 K/min. The DTG curve can easily be transformed to $\alpha(t)$ plots and then analyzed by isoconversional method (Eq. (7)) as described in Section 2.2. This method enables plotting of apparent activation energy E_a as shown in Fig. 8. Any point in this figure (corresponding to E_a for constant α) was obtained from the slope of $\ln(d\alpha/dt)$ vs. $1/T$ plot within the certain error limits (specified by bars). Similarly as it was observed for isothermal TG data also in this case the value of E_a increases with fractional conversion α

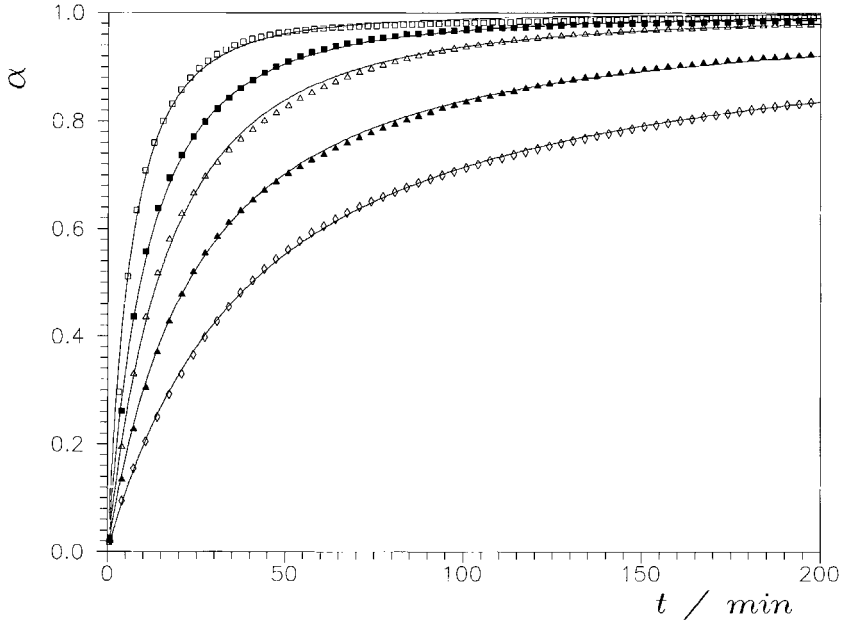

Fig. 5. Isothermal TG curves for the CY sample measured at different temperatures: (□) 380°C; (■) 370°C; (△) 360°C; (▲) 350°C; (◇) 340°C. Full lines were calculated using Eq. (13) for the kinetic parameters shown in Table 2.

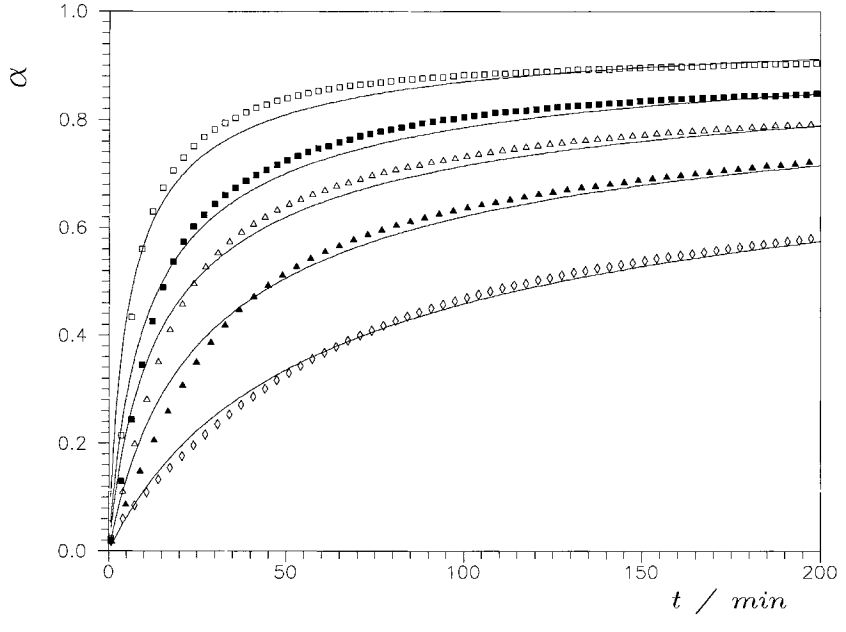

Fig. 6. Isothermal TG curves for the CYSI sample measured at different temperatures: (□) 360°C; (■) 350°C; (△) 340°C; (▲) 330°C; (◇) 320°C. Full lines were calculated using Eq. (13) for the kinetic parameters shown in Table 2.

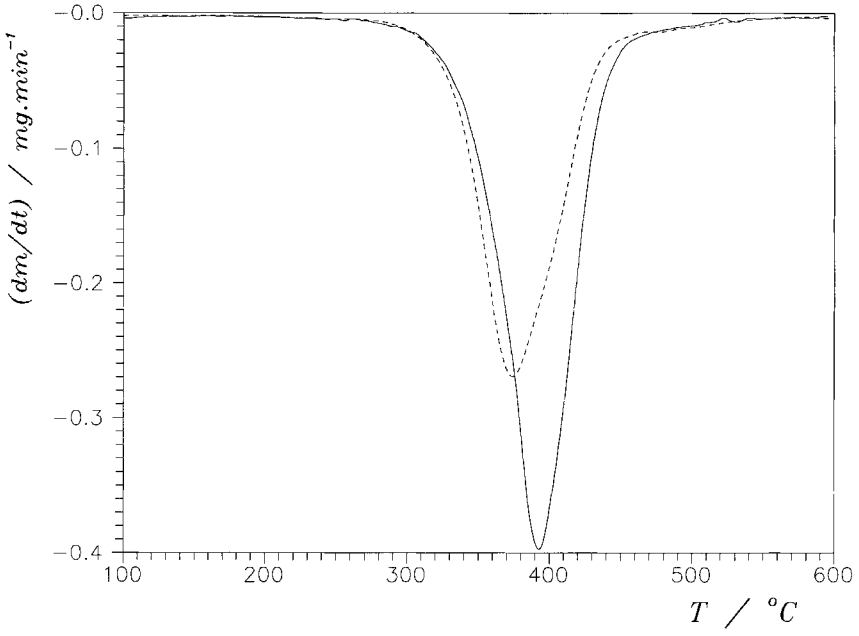

Fig. 7. Non-isothermal DTG curves for the CY sample (full line) and the CYSI sample (broken line). Heating rate: 5 K/min.

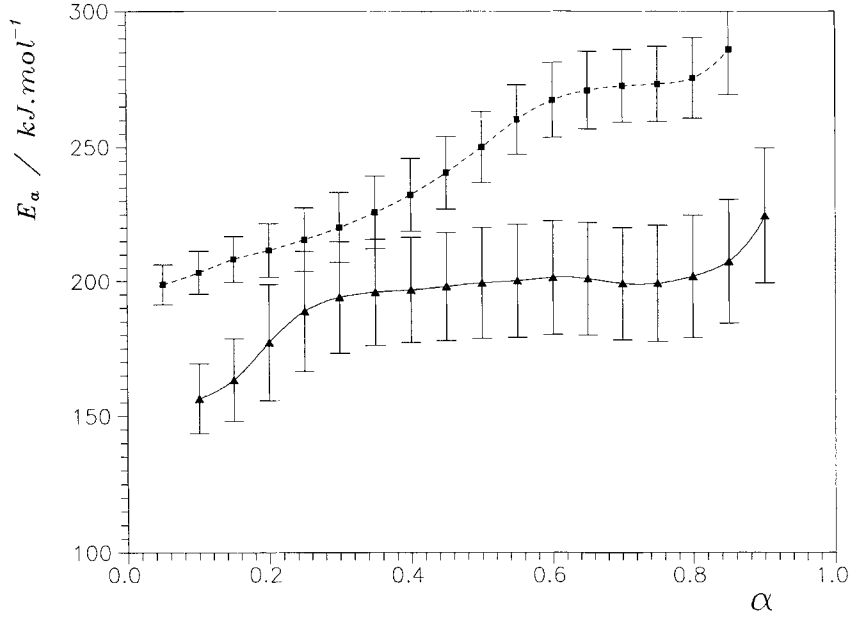

Fig. 8. The apparent activation energy calculated from non-isothermal DTG data plotted as a function of fractional conversion for the CY sample (▲) and the CYSI sample (■). The points were calculated by the isoconversional method using Eq. (7) and the lines are drawn as guide for the eye.

being higher and more α dependent for the CYSI sample. The variation of E_a in the $0.3<\alpha<0.7$ ranges is within ca. 1% for the CY sample and ca. 8% for the CYSI sample. Nevertheless, the average error limit corresponds to 10% for the CY sample and 5% for the CYSI sample, respectively. Thus, the error limit for the CY sample is ten times higher than the variation of the E_a–α plot. This fact should be taken into account when the average values of apparent activation energy is determined. The values, determined in the $0.3<\alpha<0.7$ range are 198±21 kJ/mol for the CY sample and 249±19 kJ/mol for the CYSI sample. These values are higher than the average activation energies obtained from isothermal data.

The most probable kinetic model can be determined using the $y(\alpha)$ and $z(\alpha)$ functions (Section 2.2). These functions were obtained from non-isothermal experimental ($d\alpha/dt$) data using Eqs. (11) and (12) and they are shown in Figs. 9 and 10 for CY and CYSI sample, respectively. The shape of the $z(\alpha)$ function is practically invariant with respect to temperature. In both cases, the $y(\alpha)$ function is concave (see inset in Fig. 9) and the maxima of $z(\alpha)$ function is $\alpha_p^{\infty} < 0.6$. The most probable kinetic model is, therefore, RO($n>1$) model. If the kinetic model is known the equation for non-isothermal $\alpha(T)$ curve can be obtained from Eq. (8). For the RO model, it can be written in the following form:

$$\alpha(T) = 1 - \left[1 - T\left(\frac{\pi(x)}{\beta}\right)(1-n)\mathrm{A}e^{-x}\right]^{1/(1-n)} \tag{15}$$

The temperature dependence of the reduced activation energy ($x=E_a/RT$) can easily be calculated for average value of apparent activation energy obtained by isoconversional analysis (see above). The values of parameters n and A can be obtained by non-linear regression of experimental data. The average values obtained for both CY sample and CYSI are shown in Table 3. Similarly, as discussed for isothermal data the values of pre-exponential factor and activation energy are higher for CYSI sample. The value of kinetic exponent n is also considerably higher for the CYSI than for the CY sample. Using the Eq. (14) the limiting values of α_p^{∞} were calculated for the kinetic exponent within the error limits determined from data

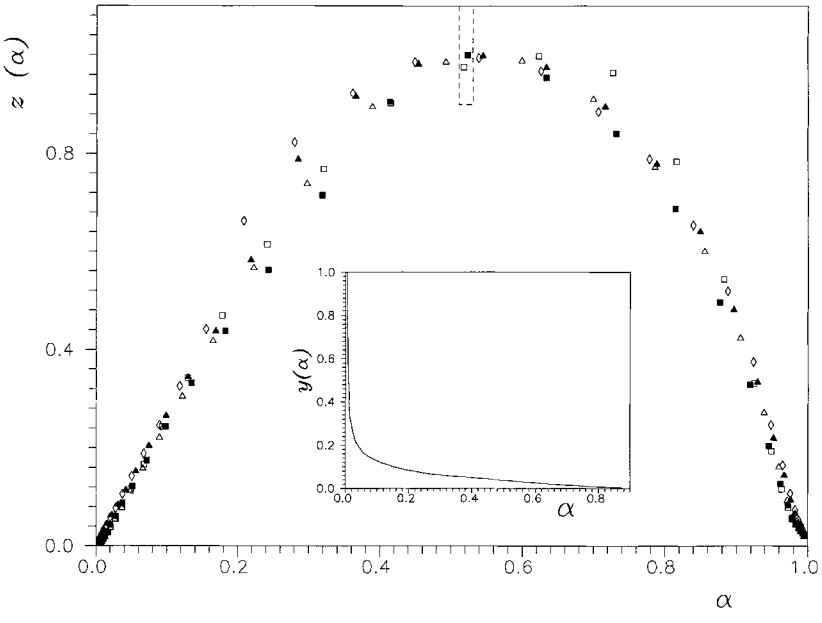

Fig. 9. The $z(\alpha)$ function for the CY sample calculated using Eq. (11) for various non-isothermal experiments: (□) 2.5 K/min; (■) 5 K/min; (△) 10 K/min; (▲) 15 K/min; (◇) 20 K/min. Broken lines correspond to theoretical maxima calculated using Eq. (14). The inset shows the $y(\alpha)$ function for the same sample calculated using Eq. (12) from experimental data corresponding to heating rate 5 K/min.

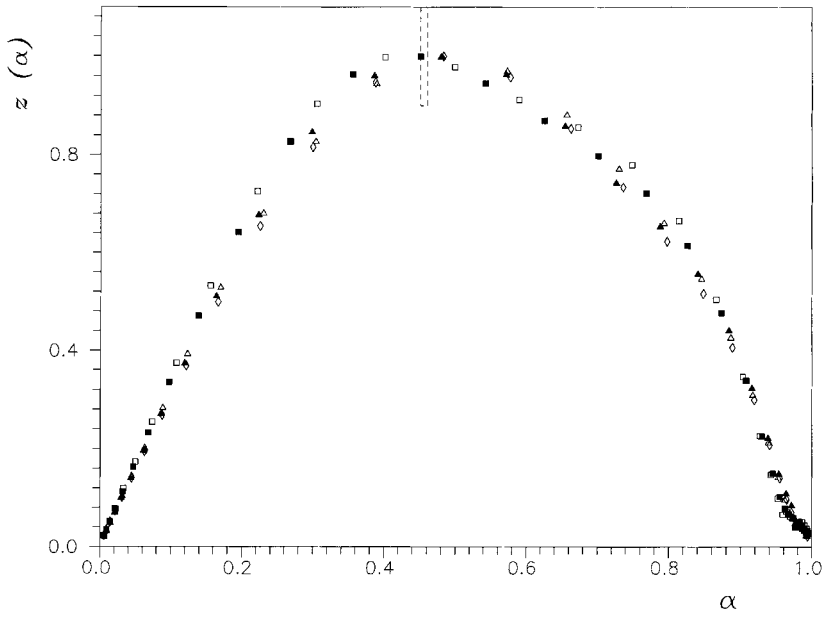

Fig. 10. The $z(\alpha)$ functions for the CYSI sample calculated using Eq. (11) for various non-isothermal experiments: (□) 2.5 K/min; (■) 5 K/min; (△) 10 K/min; (▲) 15 K/min; (◇) 20 K/min. Broken lines correspond to theoretical maxima calculated using Eq. (14).

Table 3
The kinetic parameters obtained by non-linear regression of non-isothermal data using Eq. (15) and constant value of activation energy (198 kJ/mol for the CY sample and 249 kJ/mol for the CYSI sample

	CY		CYSI	
β/K min^{-1}	n	ln(A/min)	n	ln(A/min)
2.5	2.01	34.75	2.93	45.55
5	1.74	34.52	2.83	45.33
10	1.77	34.55	2.57	44.95
15	1.58	34.41	2.55	45.15
20	1.60	34.47	2.50	44.94

shown in Table 3. These calculated limiting values are compared (broken lines) with the experimental $z(\alpha)$ function (points) in Figs. 9 and 10. There is quite good agreement between maxima of experimental $z(\alpha)$ functions and values calculated from Eq. (14).

Figs. 11 and 12 show the comparison of experimental data (points) calculated $\alpha(T)$ plots for the CY and CYSI sample (full lines). The $\alpha(T)$ curves were calculated using Eq. (15) for the kinetic parameters shown in Table 2. There is quite good agreement between experimental data and the prediction of the RO model. Some discrepancies are observed only at lower temperatures for slow heating rates. For the CYSI sample, the $\alpha(T)$ curve is shifted to lower temperatures for a given heating rate. This behavior is consistent with higher value of activation energy and the kinetic exponent n for the CYSI sample. The results clearly indicate that the silica filler reduces the thermal stability of epoxy resin studied though these are relatively minor changes. Similarly, effects of incorporation of different fillers into the thermal degradation of polyester resins have recently been described [15].

4.3. *Differences in isothermal and non-isothermal kinetics*

All kinetic results obtained in this work are consistent with a thermal degradation described by a 'reaction-order' model which can be expressed as Eq. (13) in isothermal conditions and as Eq. (15) in non-isothermal conditions. Average kinetic parameters obtained by the analysis of our experimental data are summarized in Tables 4 and 5. There is a

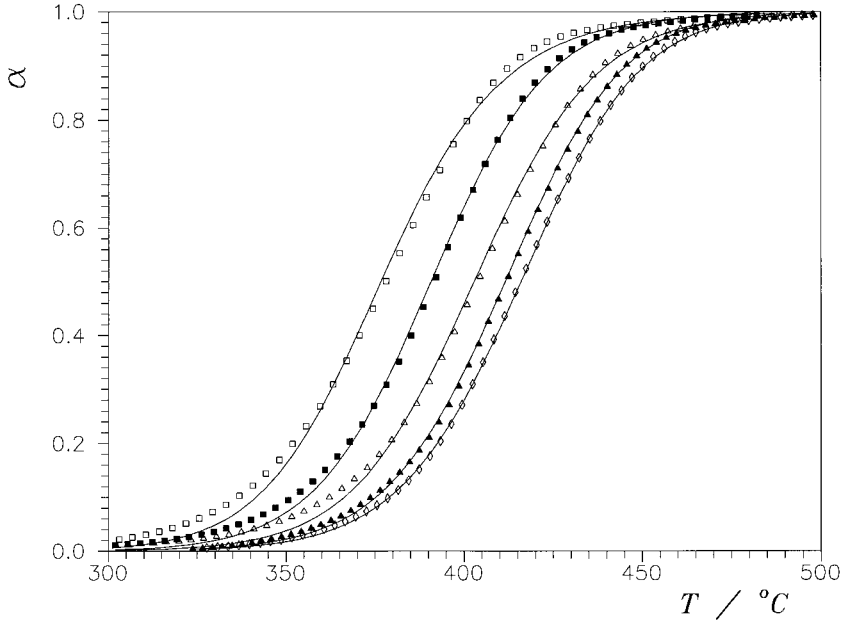

Fig. 11. Non-isothermal TG curves for the CY sample measured at different heating rates: (□) 2.5 K/min; (■) 5 K/min; (△) 10 K/min; (▲) 15 K/min; (◇) 20 K/min. Full lines were calculated using Eq. (15) for the kinetic parameters shown in Table 3.

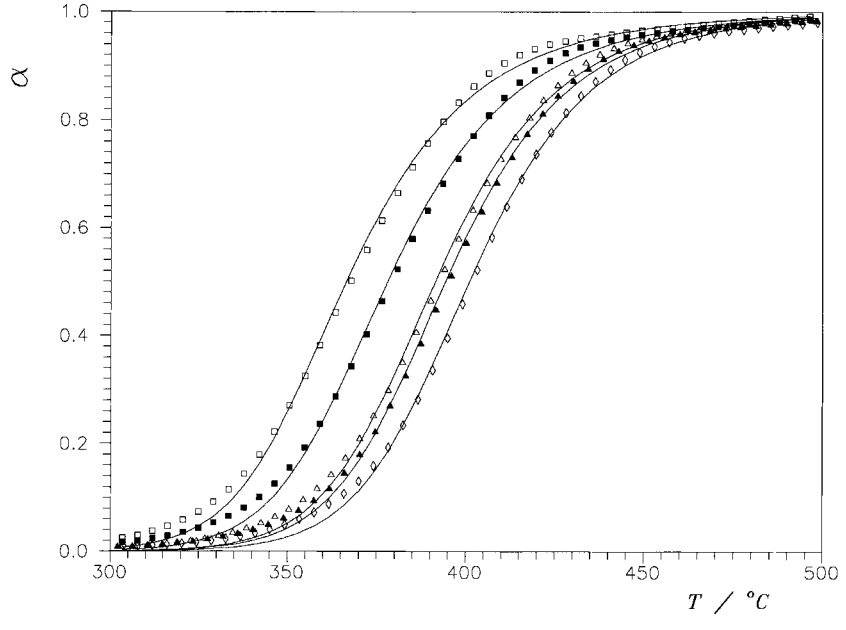

Fig. 12. Non-isothermal TG curves for the CYSI sample measured at different heating rates: (□) 2.5 K/min; (■) 5 K/min; (△) 10 K/min; (▲) 15 K/min; (◇) 20 K/min. Full lines were calculated using Eq. (15) for the kinetic parameters shown in Table 3.

Table 4
The average kinetic parameters of thermal degradation of epoxy resins CY and CYSI obtained from analysis of isothermal data

Material	E_a/kJ mol^{-1}	n	ln(A/min)
CY	173±12	1.7±0.2	30.1±0.1
CYSI	202±26	3.1±0.1	36.8±0.1

Table 5
The average kinetic parameters of thermal degradation of epoxy resins CY and CYSI obtained from analysis of non-isothermal data

Material	E_a/kJ mol^{-1}	n	ln(A/min)
CY	198±21	1.7±0.2	34.5±0.1
CYSI	249±19	2.7±0.2	45.2±0.2

difference in the value of activation energy (higher than 15%) determined from isothermal and non-isothermal experiments which cannot be explained by uncertainties typical for this type of analysis of experimental data. The value of kinetic exponent n obtained from isothermal and non-isothermal data is practically the same for the CY sample. In contrast a lower value of n is obtained for the CYSI sample from non-isothermal experiments. Therefore, it seems that the thermal decomposition kinetics of epoxy resins studied cannot be described by a unique set of kinetic parameters valid in isothermal and non-isothermal conditions. From this point of view the situation is quite different than it was found for the curing reaction kinetics [16].

5. Conclusions

From the analysis of isothermal and non-isothermal TG data, it is possible to arrive at the following general conclusions. The addition of silica filler increases thermal degradation rate of the resin and, probably, leads to a more complex mechanism of the process as compared with pure epoxy resin. The kinetics of thermal degradation can be fairly described by a simple reaction-order model. The calculated kinetic parameters are considerably lower for pure resin than for resin containing silica filler. A difference was also observed between the set of kinetic parameters obtained by kinetic analysis of isothermal and non-isothermal data, particularly with respect to the average value of apparent activation energy and the E_a–α plots.

A further study is in progress to analyze the effect of a reactive diluent on the thermal degradation kinetics of epoxy resins.

Acknowledgements

Financial support for this work has been provided by DGICYT (Project no. PB93/1241). J.M. wish to acknowledge financial assistance for a sabbatical period at UPC from the Ministerio de Educación y Ciencia.

References

[1] J. Šesták, Thermophysical Properties of Solids, Their Measurements and Theoretical Analysis, Elsevier, Amsterdam, 1984.
[2] N. Sbirrazzuoli, D. Brunel, J. Elegant, J. Thermal. Anal. 38 (1992) 1509.
[3] R.K. Agrawal, Thermochim. Acta 203 (1992) 93.
[4] R.K. Agrawal, Thermochim. Acta 203 (1992) 111.
[5] F. Carrasco, Thermochim. Acta 213 (1993) 115.
[6] P. Budrugeac, Thermochim. Acta 221 (1993) 229.
[7] R.K. Bansal, R. Agarwal, Angew. Makromol. Chem. 127 (1984) 43.
[8] J. Málek, Thermochim. Acta 138 (1989) 337.
[9] J. Málek, Thermochim. Acta 200 (1992) 257.
[10] J. Málek, V. Smrčka, Thermochim. Acta 186 (1991) 153.
[11] H.L. Friedman, J. Polym. Sci. C6 (1964) 183.
[12] G.I. Senum, R.T. Yang, J. Therm. Anal. 11 (1977) 445.
[13] J. Málek, Thermochim. Acta 267 (1995) 61.
[14] J. Málek, J.M. Criado, J. Šesták, J. Militký, Thermochim. Acta 153 (1989) 429.
[15] S.J. Evans, P.J. Haines, G.A. Skinner, Thermochim. Acta 291 (1997) 43.
[16] S. Montserrat, J. Málek, Thermochim. Acta 228 (1993) 47.